Trees, Forests and People 15 (2024) 100464

Contents lists available at ScienceDirect

Trees, Forests and People

journal homepage: www.sciencedirect.com/journal/trees-forests-and-people

Post-fire assessment of recovery of montane forest composition and stand parameters using in situ measurements and remote sensing data

Diana L. Tesha [a,*], Sami D. Madundo [b], Ernest W. Mauya [b]

[a] Department of Ecosystems and Conservation, Sokoine University of Agriculture, P. O. Box 3010, Morogoro, Tanzania
[b] Department of Forest Engineering and Wood Sciences, Sokoine University of Agriculture, P. O. Box 3014, Morogoro, Tanzania

ARTICLE INFO

Keywords:
Analysis of similarity
Generalized linear modelling
Textures
Tropical montane forests
Wildfire recovery

ABSTRACT

Tree diversity in the tropical forests face escalating threats from wildfires. This study assessed post-fire impacts and recovery patterns in Tanzanian Eastern Arc Mountains forests from 2017 to 2022 using field measurements and remote sensing techniques. Tree species diversity, composition, and forest stand parameters were compared between burned and unburned forest plots across two reserves. A predictive model utilizing 14 key variables derived from multispectral satellite data was developed to accurately map burned areas and spatial fire patterns. Results revealed significantly lower tree density, aboveground biomass, species richness, and Shannon diversity in burned areas compared to unburned forests. However, compositional analysis showed extensive species overlap between burned and unburned sites, with burned areas containing more indicative pioneer and disturbance-adapted species such as *Apodytes dimidiata*. Over time since fire events, tree density, basal area, aboveground biomass, species richness, evenness, and diversity increased markedly, evidencing active tree recovery. The remote sensing model effectively delineated approximately 1430 hectares of burned areas concentrated near villages, suggesting prevalent anthropogenic fire ignitions. Although wildfires substantially impacted forest structure and biodiversity, the limited compositional shifts point to resilience of these tropical montane forests. Integration of diverse spectral bands and textural metrics from multispectral satellite data can support precise mapping of fire effects and forest recovery dynamics in these ecologically vital yet threatened ecosystems, aiding conservation and management. Overall, this study provides novel insights into post-fire responses in Eastern Arc Mountain forests using a synergistic field and remote sensing approaches.

1. Introduction

Tropical montane forest ecosystems, characterized by their unique ecological attributes and intricate biodiversity, occupy a pivotal position in the global natural (Rurangwa et al., 2021). These ecosystems, often situated at higher altitudes, harbour a diverse array of flora and fauna species that are endemic to the specific conditions of these regions (Pinedo-Escatel et al., 2021). As repositories of diverse life forms, these forests not only contribute to the overall biodiversity of our planet but also offer vital ecosystem services, including carbon sequestration, soil stability, and provision of habitats for numerous species (Imbert et al., 2021). The imperative of conserving forests, particularly in tropical and montane regions, is deeply underlined by the complex functions they fulfill. Beyond their ecological significance, these forests play a crucial role in supporting local communities, providing essential resources, and even influencing regional climatic patterns (Imbert et al., 2021). However, in the face of escalating anthropogenic pressures, such as deforestation, land-use changes, and more prominently, fires, the integrity of these vital ecosystems is increasingly compromised (Santos Rodrigues, 2020).

The global landscape of forest ecosystems is deliberately affected by and linked to fire dynamics, with human-induced fires emerging as a potent and pervasive threat especially in the tropical montane ecosystems (Shuman et al., 2022; Tyukavina et al., 2022). The impact of fires on the achievement of REDD+ (Reducing Emissions from Deforestation and Forest Degradation) goals and carbon storage are profound, exerting a significant influence on global climate change mitigation efforts (Fawzy et al., 2020). REDD+ initiatives aim to restrict carbon emissions by conserving and sustainably managing forests, recognizing their pivotal role in carbon sequestration (Shin et al., 2022). However, the occurrence of fires, particularly in tropical and montane forest ecosystems, can disrupt this delicate equilibrium.

* Corresponding author.
E-mail address: diana.tesha@sua.ac.tz (D.L. Tesha).

https://doi.org/10.1016/j.tfp.2023.100464

Available online 13 November 2023

Fires release substantial carbon stored within trees and vegetation, contributing to atmospheric greenhouse gas concentrations (Singh, 2022). This not only negates the progress made in carbon storage through forest conservation but also worsens climate change impacts (Bowman et al., 2020). Furthermore, a study by Prichard et al. (2021) suggested that, fires alter forest structural attributes, impeding regeneration and potentially transforming forests into carbon sources instead of sinks. Therefore, effective fire management and mitigation strategies are essential to safeguard the accomplishments of REDD+ initiatives and to ensure the preservation of vital carbon reservoirs in forests, thereby contributing significantly to global climate change mitigation objectives (Tyukavina et al., 2022). The aftermath of a fire event in a forested landscape can greatly influence a wide range of ecological changes that reverberate may have implications on the entire ecosystem (Riley and Loehman, 2016). Understanding the patterns of recovery in the wake of such disturbances is of paramount importance for effective conservation and management (González, 2005).

The influence of fire on biodiversity, forest structure, and ecosystem composition can be profound, potentially leading to shifts in species dominance, alterations in vegetation dynamics, and modifications in habitat availability (Han et al., 2018). Within this context, the case of Tanzania is of particular significance, given its richness in forest types, including tropical montane forests, and the associated challenges posed by fires that disrupt these ecosystems' natural equilibrium.

The crucial role of remote sensing technologies in advancing fire ecology studies is exemplified by the potent attributes of PlanetScope and Sentinel-2 satellites (Han et al., 2021; Fernández-Guisuraga et al., 2019). These satellites, equipped with a versatile array of capabilities, offer a unique toolkit for comprehensively investigating fire occurrences, their ecological impacts, and subsequent recovery processes (Han et al., 2021). PlanetScope satellites, renowned for their high-resolution multispectral imagery, empower researchers to investigate the details of fire-affected landscapes (Dempewolf et al., 2007). The availability of various spectral bands, including near-infrared, red, and green, facilitates the computation of indices such as the Normalized Burn Ratio (NBR) and Enhanced Vegetation Index (EVI), pivotal for assessing burn severity, revealing post-fire vegetation health (Holden et al., 2010; João et al., 2018), and capturing changes in land cover and land use contributes to the understanding of long-term ecosystem responses to fires (Burton et al., 2019). This temporal dimension enables the assessment of recovery rates, the identification of lagged responses in different vegetation types, and the observation of secondary ecological effects beyond the immediate post-fire period. Sentinel-2 satellite imagery, on the other hand, provides a wealth of multispectral data, including red-edge and shortwave infrared bands, which, when coupled with texture analysis techniques, uncover fine-scale heterogeneity in burned landscapes (Hill, 2013). Texture measures, like the variance, contrast, and mean, enhance the detection of nuanced fire impacts and vegetation regeneration patterns (Lu et al., 2008).

Therefore, this study intends to unravel the complex aspects of post-fire recovery in tropical montane forests by adopting a multifaceted approach that combines field-based measurements with cutting-edge remote sensing techniques. The specific objectives of this study are to study the following; (i) effect of fire on tree species composition, (ii) effects of fire on tree species diversity and stand parameters (iii) post-fire recovery of tree species diversity and stand parameters, and (iv) estimate and map burned areas of the study sites. By investigating the trajectories of tree composition, diversity and stand parameter reconfiguration in the aftermath of fires, this study contributes valuable insights into the forest fires and trees composition relationships in the Eastern Arc Mountains especially the West Usambara montane forests ecosystems. Moreover, the role of remote sensing, particularly through platforms like PlanetScope and Sentinel-2, in monitoring fire occurrences, assessing their impact, and guiding conservation strategies, is central to this exploration.

2. Methodology

2.1. Study sites

The West Usambara Montane Forests, located in Tanzania's Lushoto and Korogwe Districts, are part of the Eastern Arc Mountains (EAMs) and consist of two highland blocks: East Usambara (up to 1484 m) and West Usambara (almost 2294 m). Our study focuses on the Magamba Nature Forest Reserve (MNFR) and the Shagayu Forest Reserve (SFR) in the West Usambara block (Fig. 1). MNFR covers 9283 hectares at 1650–2300 m above sea level, with a mean annual rainfall of 1200 mm and temperatures between 15 °C and 30 °C. SFR spans 7830 hectares at approximately 2098 m above sea level, with an annual rainfall of 1000 mm. These reserves feature a unique montane climate that supports dominant tree species like *Ocotea usambarensis, Podocarpus latifolius, Albizia gummifera, Hagenia abyssinica, Syzygium guineense*, and *Ilex mitis* (Lovett, 1996). Both reserves experience a notable fire regime, primarily from September to January, significantly influencing their dynamic montane forest ecosystems (Kilawe et al., 2021).

2.2. Study design

In this study, vegetation attributes were recorded in the Magamba Nature Forest Reserve (MNFR) and the Shagayu Forest Reserve (SFR) using a two-phase systematic sampling approach. In the first phase, a grid of sampling plots was established, with 225 × 450 m spacing in the MNFR and 350 × 700 m spacing in the SFR. During the field expedition (second phase), accessible plots from the grid intersections were selected as field sampling sites.

2.3. Data collection

2.3.1. Field data collection

In total, we established 195 circular field-sampling plots, with 90 in MNFR and 105 in SFR. Within each plot, all trees with a diameter at breast height (DBH) $\geq$ 5 cm were identified to species level and recorded. To provide a comprehensive assessment of the forest, we measured the height of three representative trees within each plot, specifically the smallest, medium-sized, and largest tree based on DBH using a vertex hypsometer. Plot locations were documented at the centre of the plot using a handheld Garmin 73 GPS device with 5 m accuracy. Additionally, we determined the status of each plot (burned or unburned) and the year of the fire event (ranging from 2022 to 2017) based on documented records on the fire occurrences in the study sites. Signs of fire disturbance, such as charred tree trunks, scorched vegetation, and fire-damaged ground cover, were also considered in this determination. Notably, data on climbers, shrubs, or herbs were not collected.

2.3.2. Sentinel-2 data acquisition and pre-processing

We acquired two Level 1C Sentinel-2 image tiles from the Copernicus Open Access Hub (https://scihub.copernicus.eu/dhus) both dated on October 12, 2022. These images were initially in Level-1C top of the atmosphere (TOA) reflectance format. Using the ESA Sen2Cor algorithm, we transformed them into Level-2A bottom of the atmosphere (BOA) surface reflectance images, employing the "sen2r" package (Ranghetti et al., 2020). We selected bands with 10 m and 20 m spatial resolutions, with the 20 m bands resampled to 10 m for spatial consistency. To cover our study area, we mosaicked the two tiles. Additionally, we sourced PlanetScope imagery for the month of October 2022, which is accessed in a pre-processed and ready for analysis form. To match our projection requirements, we re-projected the Sentinel-2 and PlanetScope data to Arc 1960 UTM 37/S (EPSG 21,037).

After data preparation, atmospherically corrected images from both sensors were used to compute vegetation indices (Table A1). We employed the "RStoolbox" package (Leutner et al., 2017), integrated into R, for this analysis. This included five fire-based vegetation indices

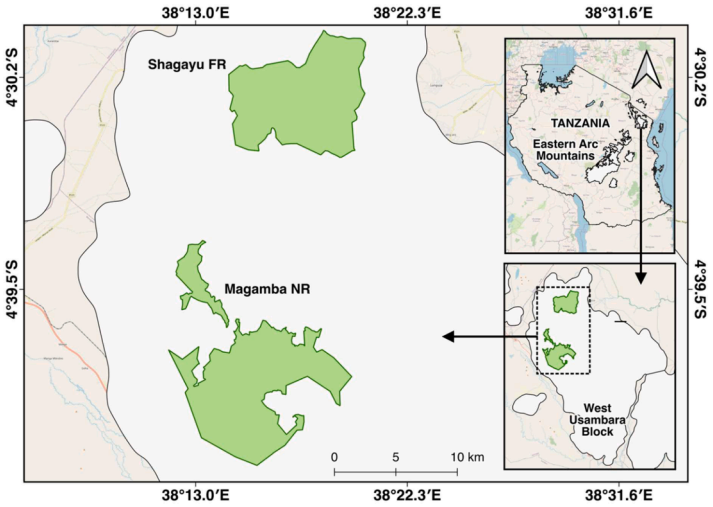

Fig. 1. Location of the study forests, in the Eastern Arc Mountains of Tanzania.

(Alcaras et al., 2022), five broadband optical vegetation indices, and three narrowband indices specific to Sentinel-2 data. Furthermore, we calculated grey level co-occurrence matrix (GLCM) textural metrics - 'mean,' 'variance,' and 'dissimilarity' - across all spectral bands and indices. This texture analysis, performed with the "glcm" package in R (Zvoleff, 2020), used a 3 × 3 window size to capture spatial patterns within the imagery.

2.4. Statistical analyses

Tree species composition: To determine significant differences in tree species composition between burned and unburned sites, a non-metric multidimensional scaling analysis (NMDS) using a Bray-Curtis dissimilarity coefficient and analysis of similarity of the abundance matrix (ANOSIM) with P value of 0.05 were used (Huang et al., 2016). By ordinating sites based on their species compositions, the NMDS enabled the visual assessment of whether burned and unburned forest sites differ systematically based on their species abundances. NMDS provided an unconstrained visualization of the patterns in this complex dataset, complementing the ANOSIM results to understand differences between burned and unburned conditions. Only tree species with an abundance of more than 5 individuals were used for the analyses. The ANOSIM calculates the differences of the ranked dissimilarities between and within a-priori specified groups. This method calculates an R value that can be interpreted as the amount of overlap of the groups in multivariate space. *R* values range from 0 to 1, with values less than 0.5 indicating strong overlap and values of more than 0.75 indicating clearly different clusters in multivariate space (Anderson and Walsh, 2013). Indicator species analysis was then performed to identify significant associations of tree species to burned and unburned sites based on indicator value. The NMDS and ANOSIM analysis were implemented using the 'vegan' R package v2.6-4 (Oksanen et al., 2007), while indicator species analysis was conducted using the 'indicspecies' R package (De Caceres et al., 2016).

Tree diversity, stand parameters and recovery: To determine the relationship between wildfire and forest diversity, stand parameters and their recovery over time, we calculated for all plots; density (N, total number of trees ha^{-1}), basal area (G, m^2ha^{-1}), above-ground biomass (AGB, $Mgha^{-1}$), species richness (S, total number of species per plot), Pileous evenness (J), and species diversity expressed as Shannon's index (H'). Prior to analysis, these parameters were tested for normality, revealing that they were not normally distributed. Generalized linear models (GLMs) were used to analyse whether fire (burned vs unburned) had a significant impact on the forest diversity and stand parameters (Butler et al., 2017). For the six different models based on each specific parameter, the following families and link functions were employed: a Gaussian family with log link for both density and above-ground biomass, a gamma family with a log link for basal area, and a Poisson family and log link for species richness, evenness, and diversity. All forest diversity and stand parameters that were significantly influenced by fire were then compared between burned and unburned forest sites to quantify effects using Mann-Whitney *U* tests. Spearman correlations were calculated between all forest diversity and stand parameters and time since fire occurrence to determine if the parameters recover over time (Armenteras et al., 2021).

Fire mapping: A predictive model was developed for mapping the most recent burned forest areas using the Sentinel-2 and PlanetScope spectral bands, vegetation and burn indices, and textures. We employed XGBoost, a powerful machine learning algorithm, using a training dataset containing both burned and unburned plot locations under k-fold cross-validation ($k = 10$). To enhance model accuracy and efficiency, we conducted an in-depth analysis of variable importance using Recursive Feature Elimination (RFE) (Zhang et al., 2022). RFE allowed us to iteratively identify the most influential predictors which were then used to create a final optimised model to generate a detailed burned area map of the study forests.

3. Results

3.1. Post-fire effects on tree species composition

The results of the ANOSIM analysis showed that there are no clear groups formed by the effects of wildfires (ANOSIM-$R = 0.11$). These results were significant at the 95 % significance level after 999 permutations (Fig. 2). This demonstrates a strong overlap of forest species composition. On the other hand, indicator species analysis revealed that 21 of the 195 species significantly occurred across the sites respectively (Table 1). We found a total of 13 species, including *Apodytes dimidiata* E. Mey. ex Arn. and *Canthium captum* Bullock, occurred in burned sites. In unburned sites, *Cyathea manniana* Hook. was the most indicative species. Generally, more species were indicative of burned areas compared to unburned areas (Table 1).

3.2. Post-fire effects on tree diversity and stand parameters

Fire was found to have an effect on all stand and diversity parameters with the exception of species evenness (Table 2). Focusing on tree parameters with significant effects by fire, we compared them between burned and unburned areas of the forests. As shown in Table 3, all included parameters were found to differ significantly between burned

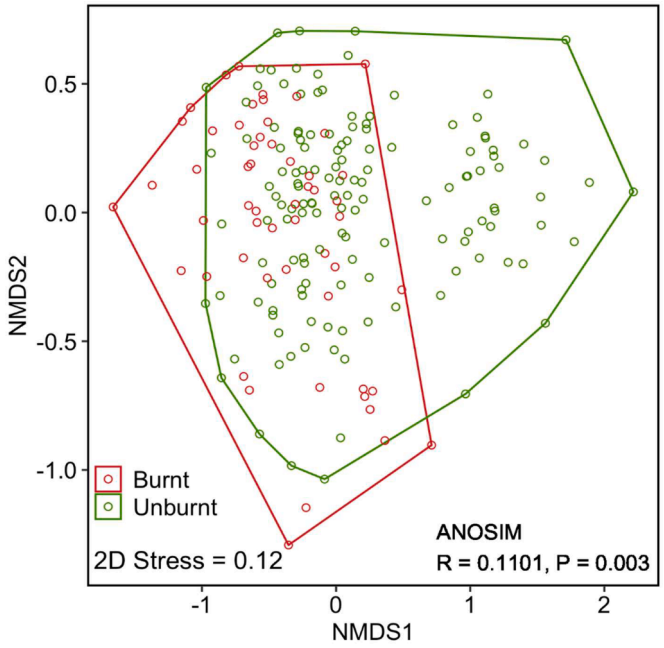

Fig. 2. Non-metric multidimensional scaling ordination (NMDS) for forest plots showing convex hulls.

and unburned forest areas. The tree density was 38.4 % lower after fire disturbance, as was the basal area (41.7 %). In addition, we found about 52.2 % fewer species in burned forests as compared to unburned forests. The comparison of species diversity between burned and unburned forests showed that there was 31.3 % less species diversity (H') in burned forests.

3.3. Post-fire recovery of tree diversity and stand parameters

In our study, we found strong and statistically significant positive correlations between years since fire disturbance and all tree diversity and stand parameters (Fig. 3). Tree density increased significantly with time since fire ($P = >0.001$, $r = 0.49$), as did basal area ($P = >0.001$, $r = 0.58$), and above-ground biomass (AGB) ($P = >0.001$, $r = 0.6$). The Shannon diversity index exhibited a highly significant positive correlation ($P = >0.001$, $r = 0.87$), indicating an increase in species diversity over time. Similarly, species richness showed a remarkable increase ($P = >0.001$, $r = 0.95$), accompanied by a significant positive correlation with years since fire. Evenness also displayed a positive correlation ($P = 0.003$, $r = 0.39$) with time since fire, albeit with a lower coefficient.

3.4. Burned area mapping

Through Recursive Feature Elimination (RFE), we identified an optimal model comprising 14 key predictor variables that effectively captured post-fire landscape dynamics for the study sites. Notable variables in this selection included the contrast of NBRplus, the mean texture of Sentinel-2 red band (B04), PlanetScopes DVI and others (Fig. 4).

The optimised model demonstrated robust performance, with an accuracy of 0.688 (SD: 0.083) and a kappa value of 0.0998 (SD: 0.261), showing its ability to distinguish burned and unburned areas accurately (Table A2). Using the model, a burned area prediction map was created to visually depict the spatial distribution of burned areas (Fig. 5). From the map a total burned area of approximately 1430 hectares was found.

4. Discussion

The findings of this study point to a degree of ecological resilience of

Table 1
Indicator species analysis for the burned and unburned sites of the forests.

Site status	Scientific name	Code	Importance value	*P*-value
Burned	*Apodytes dimidiata* E.Mey. ex Arn.	Apo. dim	0.438	0.010
	Canthium captum Bullock	Can. cap	0.339	0.003
	Cussonia holstii Harms ex Engl.	Cus. hol	0.326	0.045
	Diospyros natalensis (Harv.) Brenan	Dio. nat	0.268	0.039
	Euclea divinorum Hiern	Euc. div	0.472	0.001
	Maytenus senegalensis (Lam.) Exell	May. sen	0.416	0.002
	Mystroxylon aethiopicum (Thunb.) Loes.	Mys. aet	0.453	0.001
	Ochna holstii Engl.	Och. hol	0.443	0.011
	Olea europaea subsp. africana (Mill.) P.S.Green	Ole. eur	0.339	0.005
	Olinia rochetiana A.Juss.	Oli. roc	0.386	0.004
	Rhus natalensis Bernh. ex C. Krauss	Rhu. nat	0.379	0.004
	Trichocladus ellipticus Eckl. & Zeyh.	Tri.ell	0.464	0.018
	Warburgia ugandensis Sprague	War. uga	0.281	0.026
Unburned	*Cyathea manniana* Hook.	Cya. man	0.835	0.001
	Dasylepis integra Warb.	Das. int	0.417	0.049
	Ehretia cymosa Thonn.	Ehr. cym	0.231	0.024
	Entandrophragma excelsum (Dawe & Sprague) Sprague	Ent. exc	0.244	0.018
	Leptonychia usambarensis K. Schum.	Lep. usa	0.332	0.007
	Margaritaria discoidea (Baill.) G. L.Webster	Mar. dis	0.239	0.030
	Mussaenda microdonta Wernham	Mus. mic	0.388	0.001
	Turraea holstii Gürke	Tur. hol	0.333	0.004

Table 2
Influence of fire on tree density, basal area, above-ground biomass, species richness, evenness, and diversity, mean with standard error (SE) of all 195 plots (N) (burned and unburned), and *P*-values.

Stand/Diversity parameter	*N*	Mean (SE)	Fire influence
Tree density (N, trees ha^{-1})	195	651.87 ± 29.19	>0.001
Basal area (G, m^2ha^{-1})	195	25.78 ± 1.66	0.002
Above-ground biomass (AGB, $Mgha^{-1}$)	195	255.54 ± 15.85	>0.001
Species richness (S)	195	12.77 ± 0.44	>0.001
Species evenness (J)	192 *	0.82 ± 0.01	0.689
Shannon diversity (H')	195	2.03 ± 0.04	0.001

* *N* is smaller, as the computation of species evenness is only possible for plots with at least two tree species.

Table 3
Differences between burned and unburned forest sites ($N = 56$ burned, $N = 139$ unburned).

Structural parameter	Unburned	Burned	*P*-value
Tree density (N, trees ha^{-1})	949 ± 66.30	585 ± 30.10	>0.001
Basal area (G, m^2ha^{-1})	39.1 ± 3.46	22.8 ± 1.80	0.002
Above-ground biomass (AGB, $Mgha^{-1}$)	393 ± 32.00	224 ± 17.10	>0.001
Species richness (S)	22.2 ± 0.56	10.6 ± 0.34	>0.001
Shannon diversity (H')	2.72 ± 0.03	1.87 ± 0.04	0.001

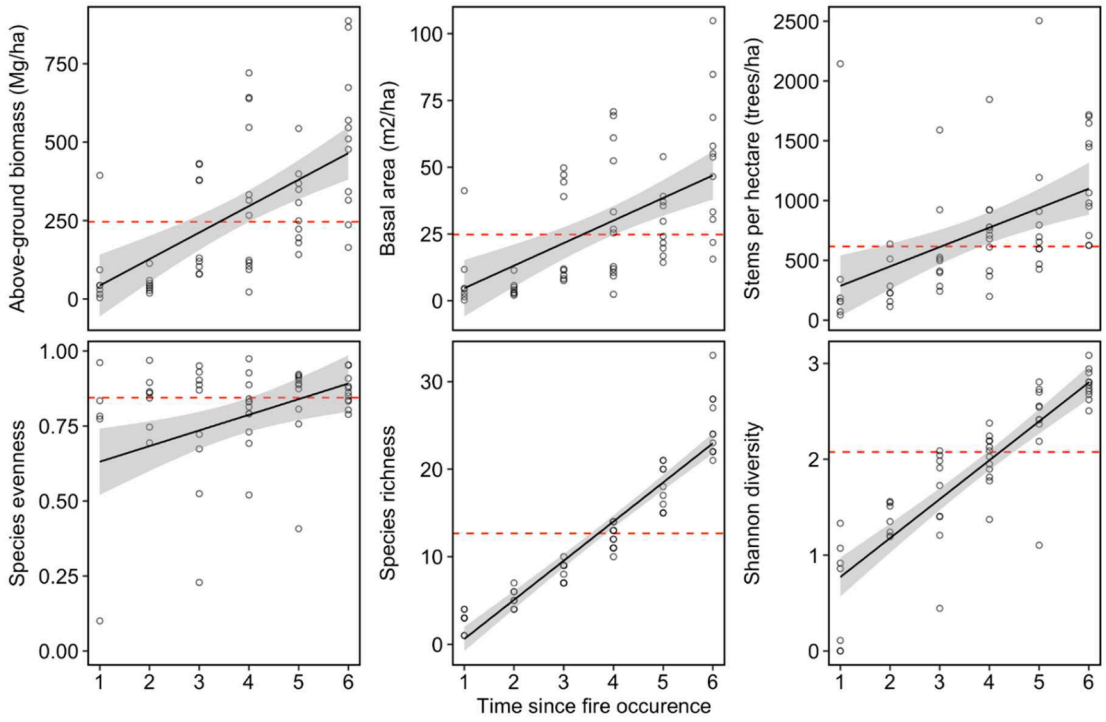

Fig. 3. Post-fire recovery of (a) above-ground biomass, (b) basal area, (c) density, (d) species evenness, (e) richness, and (f) diversity, in the forests. Dots represent plots burned in 2022 ($n = 7$), 2021 ($n = 7$), 2020 ($n = 9$), 2019 ($n = 12$), 2018 ($n = 10$), and 2017 ($n = 11$). The solid black line indicates the linear trend line of the burned forest parameter values, with 95 % confidence interval. Mean unburned tree stand parameter is indicated by the red horizontal dashed line.

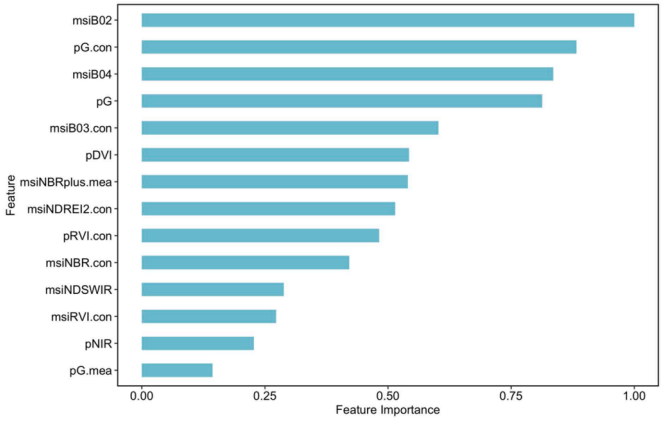

Fig. 4. Relative importance plot of optimal Sentinel-2 and PlanetScope remote sensing features in mapping burned forest areas using XGBoost. Features include: *msiB02* = Sentinel-2 band 2 (Blue), *pG.con* = contrast of PlanetScope green band, *msiB04* = Sentinel-2 band 4 (Red), *pG* = PlanetScope green band, *msiB03.con* = contrast of Sentinel-2 band 3 (Green), *pDVI* = PlanetScope difference vegetation index, *msiNBRplus.mea* = mean of Sentinel-2 NBRplus, *pRVI.con* = contrast of PlanetScope ratio vegetation index, *msiNBR.con* = contrast of Sentinel-2 normalized burn ratio, *msiNDSWIR* = Sentinel-2 normalized difference short-ware infrared burn index, *msiRVI.con* = contrast of Sentinel-2 ratio vegetation index, *pNIR* = PlanetScope near-infrared band, and *pG.mea* = mean of PlanetScope green band.

Tanzanian Eastern Arc montane forests to wildfire disturbances. Despite the significant impacts of tree species stand parameters like above-ground biomass and tree density, we found minimal shifts in overall tree species composition between burned and unburned forest areas. The extensive overlap shown by the ANOSIM analysis suggests that many dominant tropical montane tree species are able to persist through or rapidly recolonize following fires (Ford and Hardesty, 2012; Mondal and Sukumar, 2015). This aligns with other studies in tropical forests that found limited changes to fundamental tree species composition after even high-severity burns compared to more pronounced compositional shifts in temperate and boreal systems (Barlow and Peres, 2004; Oliveras et al., 2014, 2018).

Certain inherent traits like resprouting allow many tropical tree species to regenerate after fire (Teixeira et al., 2020). Our identification of disturbance-associated pioneer species as indicators in burned plots points to prevalence of fire-adapted species, although most species were shared across sites. This underscores the vital capacity of these forests to naturally restore ecological structure and functions despite disruptions (Mori et al., 2017). However, potential lags and thresholds exist – increased frequencies of fire could overcome resilience mechanisms if insufficient recovery time is allowed between burns (Wilcox et al., 2020).

Active ecological recovery processes within these tropical montane forests were shown in this study through post-fire regeneration patterns across a 5-year period. We found strong positive correlations between stand and diversity parameters like density, biomass, and Shannon's index and time since fire. This accumulation of biomass over time highlights the forests capacity to gradually restore carbon storage and sequestration functions that are central to climate change mitigation (Chazdon et al., 2016). The recovery of species diversity and richness also demonstrates the steady re-establishment of complex ecological niches and habitats (Derroire et al., 2016). However, some parameters may recover faster than others – tree density and basal area rebounded more rapidly compared to diversity (Majumdar et al., 2016; McGregory et al., 2016). Varied regeneration rates across diversity and stand parameters point to potential time lags (Subashree et al., 2020). While forests may regain simpler structural complexity shortly after fire, elements like species richness and heterogeneity may require longer undisturbed periods to fully recover (Cavallero et al., 2015).

The value of integrating multispectral remote sensing data from PlanetScope and Sentinel-2 platforms to map and analyse fire patterns in these tropical montane forests was demonstrated in this study. The

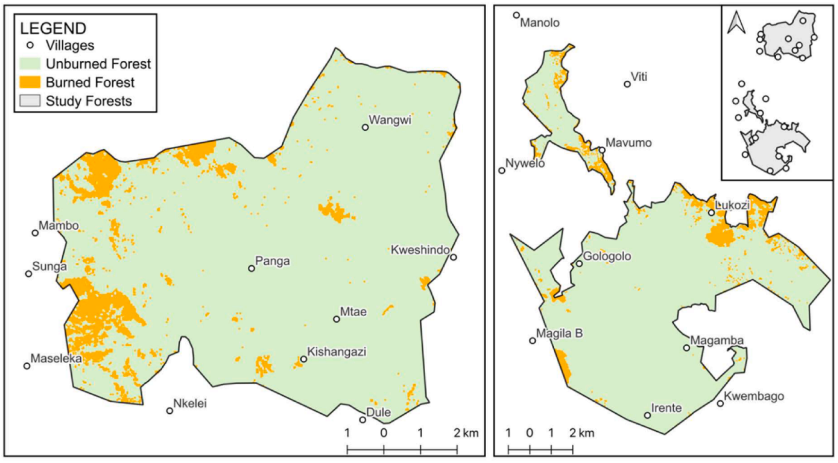

Fig. 5. Burned area prediction map for Shagayu forest reserve (left) and Magamba Nature forest reserve (right) derived from the optimised XGBoost model.

optimized predictive model accurately delineated burn areas totalling approximately 1430 hectares, with hotspots clustered near villages. This suggests prevalent anthropogenic ignitions, aligning with other tropical forest studies (Balch et al., 2008; Morris, 2010; Kelley et al., 2019). The model optimization using Recursive Feature Elimination highlighted the importance of textural metrics like contrast of NBR+ for quantifying landscape heterogeneity (Chen et al., 2018; Mishra et al., 2018). The approach also revealed the utility of diverse spectral bands and indices for capturing fire impacts on vegetation health (Bar et al., 2020; Miller and Thode, 2007). While some key predictors differed from previous tropical forest models, the overall effectiveness underscores the adaptability of this mapping methodology. The capacity to integrate datasets from multiple sensors provides a flexible toolkit to generate time-series analyses that reveal both immediate and lagged ecological responses over the post-fire recovery trajectory (Chuvieco et al., 2020).

While this study gives important insights into post-fire assessment on tree species composition, diversity, and stand parameters, there are some limitations to consider. The relatively short interval of 5 years since fire events may not capture longer-term successional dynamics. Legacy effects and cumulative impacts of previous fires, as well as other disturbances like land use changes, were not accounted for but may influence vegetation patterns. The restricted spatial scale focused on only two forest reserves, which could limit generalization. Monitoring across broader temporal and spatial scales would build understanding of recovery patterns. Despite these limitations, this work makes a significant contribution by assessing post-fire tree responses in an important region and ecosystem type while providing a foundation for further investigations into tropical montane forest dynamics.

5. Conclusion

Our study highlights post-fire effects in Eastern Arc Mountain forests using an integrative approach combining field measurements and optical remote sensing. Despite fire disturbances, the forests display extensive tree species overlap, and only slight compositional shifts were observed. Strong correlations between diversity and stand parameters with time since fire demonstrate regeneration, showing the forests capacity to reaccumulate biomass and regenerate tree diversity. The remote sensing model effectively mapped burn areas and revealed fire hotspots near villages, the utility of spectral indices and textures for monitoring wildfires. These findings have important implications for the conservation of threatened yet critical tropical montane forests. Further investigations should build on these findings, focusing on long-term monitoring, fire frequency thresholds, strategies to mitigate wildfire ignitions, and the effects on overall biodiversity of the area.

Data availability statement

The data that support the findings of this study are available from the corresponding author upon reasonable request.

CRediT authorship contribution statement

Diana L. Tesha: Conceptualization, Methodology, Data curation, Formal analysis, Writing – original draft. **Sami D. Madundo:** Formal analysis, Visualization, Writing – review & editing. **Ernest W. Mauya:** Supervision, Conceptualization, Methodology, Writing – review & editing.

Declaration of Competing Interest

The authors declare the following financial interests/personal relationships which may be considered as potential competing interests: Ernest William Mauya reports financial support was provided by Eastern Arc Mountains Conservation Endowment Fund. Diana Lawrence Tesha reports financial support was provided by Regional Centre for Mapping of Resources for Development. Diana Lawrence Tesha reports financial support was provided by Tanzania Forest Fund.

Acknowledgements

The authors would like to thank the Eastern Arc Mountains Conservation Endowment Fund (EAMCEF), the Tanzania Forest Fund (TaFF), and the Regional Centre for Mapping of Resources for Development/ Global Monitoring for Environment and Security Africa (RCMRD/GMES Africa) for their invaluable support in funding this research study.

Appendices

Table A1
Description of vegetation indices used as predictor variables for burn area mapping.

Index	Name	Expression	Sensor	Reference
DVI	Difference Vegetation Index	NIR-Red	S-2, PS	Richardson and Wiegand (1977)
EVI	Enhanced Vegetation Index	2.5[(NIR − Red) / (NIR + 2.4Red + 1)]	S-2, PS	Liu and Huete (1995)
GNDVI	Green Normalized Difference Vegetation Index	(NIR − Green) / (NIR + Green)	S-2, PS	Gitelson et al. (1996)
NDVI	Normalized Difference Vegetation Index	(NIR − Red) / (NIR + Red)	S-2, PS	Rouse et al. (1974)
RVI	Ratio Vegetation Index	NIR / Red	S-2, PS	Pearson and Milton (1972)
CLRE	Chlorophyll Red-Edge	(RE3 / RE1) − 1	S-2	Gitelson et al., 2003
ND-RE1	Normalized Difference Red Edge	(RE2 − RE1)/(RE2 + RE1)	S-2	Gitelson and Merzlyak (1994)
ND-RE2	Normalized Difference Red Edge	(RE3 − RE1) / (RE3 + RE1)	S-2	Barnes et al. (2000)
NBR	Normalized Burn Ratio	(B12 − B8A) / (B12 + B8A)	S-2	Garcia and Caselles (1991)
NBRSWIR	Normalized Burn Ratio-SWIR	(B12 − B11 − 0.02) / (B12 + B11 + 0.1)	S-2	Liu et al. (2020)
NDSWIR	Normalized Difference Shortwave Infrared Index	(B11 − B8A) / (B11 + B8A)	S-2	Gerard et al. (2003)
MIRBI	Mid-Infrared Bi-Spectral Index	10B12 − 9.8 × B11 + 2	S-2	Trigg and Flasse (2001)
BAIS2	Burned Area Index for Sentinel 2	$\left(1-\sqrt{\frac{B6\times B7\times B8A}{B4}}\right)\times\left(\frac{B12-B8A}{\sqrt{B12+B8A}}+1\right)$	S-2	Filipponi (2018)
NBR+	Normalized Burn Ration Plus	(B12 − B8A − B3 − B2) / (B12 + B8A + B3 + B2)	S-2	Alcaras et al. (2022)

Table A2
Recursive feature elimination (RFE) results under 10-fold cross-validation showing performance of feature resampling over total feature subset size (132). The row in bold indicates the optimal feature subset.

Number of features	Accuracy	Kappa	AccuracySD	KappaSD
1	0.533	−0.118	0.058	0.190
2	0.626	0.013	0.073	0.181
3	0.632	0.036	0.102	0.263
4	0.617	0.008	0.090	0.179
5	0.658	0.093	0.089	0.187
6	0.662	0.056	0.087	0.244
7	0.677	0.080	0.084	0.218
8	0.688	0.097	0.094	0.262
9	0.688	0.123	0.099	0.250
10	0.668	0.081	0.107	0.256
11	0.657	0.040	0.078	0.163
12	0.662	0.038	0.073	0.185
13	0.673	0.058	0.071	0.181
14	**0.693**	**0.140**	**0.067**	**0.155**
15	0.662	0.032	0.075	0.183
16	0.683	0.104	0.072	0.171
17	0.678	0.098	0.074	0.162
18	0.683	0.107	0.083	0.191
19	0.678	0.109	0.081	0.151
20	0.688	0.114	0.076	0.192
21	0.678	0.072	0.059	0.169
22	0.673	0.063	0.059	0.169
23	0.688	0.089	0.052	0.164
24	0.662	0.033	0.053	0.163
25	0.677	0.070	0.076	0.211
26	0.683	0.095	0.067	0.213
27	0.672	0.060	0.068	0.191
28	0.662	0.042	0.062	0.189
29	0.673	0.073	0.075	0.196
30	0.683	0.084	0.078	0.228
31	0.672	0.073	0.073	0.202
32	0.673	0.054	0.078	0.208
33	0.668	0.044	0.071	0.180
34	0.683	0.093	0.074	0.184
35	0.673	0.073	0.080	0.167
36	0.678	0.062	0.067	0.148
37	0.688	0.093	0.073	0.173
38	0.678	0.064	0.075	0.165
39	0.688	0.087	0.057	0.151
40	0.693	0.108	0.079	0.203
41	0.678	0.075	0.088	0.194
42	0.682	0.079	0.060	0.154
43	0.678	0.092	0.075	0.169
44	0.667	0.034	0.079	0.195
45	0.662	0.026	0.080	0.195
46	0.667	0.035	0.080	0.188
47	0.667	0.046	0.076	0.186

(*continued on next page*)

Table A2 (*continued*)

Number of features	Accuracy	Kappa	AccuracySD	KappaSD
48	0.657	0.017	0.079	0.200
49	0.672	0.046	0.067	0.144
50	0.672	0.042	0.072	0.184
51	0.662	0.024	0.069	0.180
52	0.657	0.017	0.079	0.200
53	0.672	0.059	0.077	0.183
54	0.667	0.033	0.070	0.174
55	0.677	0.050	0.069	0.175
56	0.683	0.060	0.071	0.169
57	0.672	0.044	0.077	0.200
58	0.672	0.042	0.072	0.184
59	0.662	0.026	0.080	0.203
60	0.672	0.046	0.087	0.206
61	0.667	0.021	0.072	0.187
62	0.678	0.067	0.075	0.181
63	0.678	0.077	0.093	0.229
64	0.673	0.054	0.088	0.228
65	0.667	0.034	0.079	0.195
66	0.662	0.026	0.080	0.203
67	0.678	0.056	0.076	0.208
68	0.677	0.063	0.073	0.199
69	0.683	0.083	0.085	0.231
70	0.667	0.034	0.079	0.195
71	0.678	0.047	0.088	0.221
72	0.667	0.046	0.073	0.181
73	0.667	0.040	0.083	0.201
74	0.652	−0.003	0.079	0.202
75	0.668	0.028	0.086	0.229
76	0.657	0.005	0.079	0.196
77	0.662	0.026	0.080	0.203
78	0.668	0.028	0.086	0.229
79	0.662	0.013	0.079	0.197
80	0.667	0.034	0.079	0.195
81	0.657	0.011	0.082	0.224
82	0.662	0.020	0.086	0.236
83	0.667	0.033	0.070	0.182
84	0.678	0.032	0.078	0.212
85	0.662	0.020	0.086	0.236
86	0.677	0.052	0.076	0.192
87	0.667	0.021	0.070	0.179
88	0.657	0.006	0.080	0.200
89	0.673	0.061	0.083	0.194
90	0.672	0.037	0.080	0.224
91	0.667	0.022	0.071	0.183
92	0.662	0.013	0.070	0.186
93	0.667	0.030	0.091	0.253
94	0.672	0.062	0.084	0.202
95	0.657	0.012	0.086	0.235
96	0.672	0.029	0.068	0.179
97	0.673	0.037	0.083	0.217
98	0.662	0.012	0.073	0.186
99	0.662	0.014	0.077	0.190
100	0.662	0.014	0.077	0.190
101	0.667	0.028	0.078	0.221
102	0.667	0.021	0.072	0.187
103	0.652	−0.003	0.079	0.202
104	0.662	0.013	0.070	0.186
105	0.682	0.078	0.077	0.203
106	0.683	0.066	0.078	0.202
107	0.662	0.020	0.086	0.229
108	0.683	0.072	0.085	0.220
109	0.667	0.026	0.070	0.225
110	0.662	0.009	0.073	0.201
111	0.667	0.026	0.070	0.225
112	0.673	0.025	0.083	0.215
113	0.683	0.072	0.080	0.227
114	0.657	0.010	0.070	0.162
115	0.662	0.013	0.096	0.239
116	0.667	0.037	0.072	0.195
117	0.667	0.021	0.072	0.187
118	0.683	0.073	0.089	0.223
119	0.667	0.041	0.084	0.206
120	0.683	0.084	0.080	0.226
121	0.652	−0.016	0.077	0.201
122	0.673	0.031	0.079	0.209
123	0.678	0.040	0.075	0.178

(*continued on next page*)

Table A2 (*continued*)

Number of features	Accuracy	Kappa	AccuracySD	KappaSD
124	0.677	0.038	0.069	0.174
125	0.672	0.060	0.081	0.214
126	0.667	0.022	0.073	0.191
127	0.682	0.060	0.069	0.183
128	0.672	0.030	0.070	0.183
129	0.672	0.047	0.090	0.229
130	0.678	0.057	0.080	0.197
131	0.672	0.018	0.056	0.156
132	0.678	0.055	0.072	0.212

References

Alcaras, E., Costantino, D., Guastaferro, F., Parente, C., Pepe, M., 2022. Normalized burn ratio plus (NBR+): a new index for Sentinel-2 imagery. Remote Sens. (Basel) 14 (7), 1727. https://doi.org/10.3390/rs14071727.

Anderson, M.J., Walsh, D.C., 2013. PERMANOVA, ANOSIM, and the Mantel test in the face of heterogeneous dispersions: what null hypothesis are you testing? Ecol. Monogr. 83 (4), 557–574.

Armenteras, D., Dávalos, L.M., Barreto, J.S., Miranda, A., Hernández-Moreno, A., Zamorano-Elgueta, C., González-Delgado, T.M., Meza-Elizalde, M.C., Retana, J., 2021. Fire-induced loss of the world's most biodiverse forests in Latin America. Sci. Adv. 7 (33), eabd3357.

Balch, J.K., Nepstad, D.C., Brando, P.M., Curran, L.M., Portela, O., de Carvalho Jr., O., Lefebvre, P., 2008. Negative fire feedback in a transitional forest of southeastern Amazonia. Global Change Biology 14 (10), 2276–2287.

Bar, S., Parida, B., Pandey, A., 2020. Landsat-8 and Sentinel-2 based forest fire burn area mapping using machine learning algorithms on GEE cloud platform over Uttarakhand, Western Himalaya. Remote Sens. Appl.: Soc. Environ. 18, 100324 https://doi.org/10.1016/j.rsase.2020.100324.

Barlow, J., Peres, C.A., 2004. Ecological responses to El Niño–induced surface fires in central Brazilian Amazonia: management implications for flammable tropical forests. Philos. Trans. R. Soc. Lond. B. Biol. Sci. 359 (1443), 367–380.

Barnes, E.M., Clarke, T.R., Richards, S.E., Colaizzi, P.D., Haberland, J., Kostrzewski, M., Waller, P., Choi, C., Thompson, T., Lascano, R.J., Li, H., Moran, M.S, 2000. Coincident detection of crop water stress, nitrogen status and canopy density using ground based multispectral data. Proceedings of the 5th International Conference on Precision Agriculture.

Bowman, D.M., Kolden, C.A., Abatzoglou, J.T., Johnston, F.H., van der Werf, G.R., Flannigan, M., 2020. Vegetation fires in the Anthropocene. Nat. Rev. Earth Environ. 1 (10), 500–515.

Burton, C., Betts, R., Cardoso, M., Feldpausch, T.R., Harper, A., Jones, C.D., Kelley, D.I., Robertson, E., Wiltshire, A., 2019. Representation of fire, land-use change and vegetation dynamics in the joint UK land environment simulator vn4.9 (JULES). Geosci. Model Dev. 12 (1), 179–193. https://doi.org/10.5194/gmd-12-179-2019.

Butler, O.M., Lewis, T., Chen, C., 2017. Prescribed fire alters foliar stoichiometry and nutrient resorption in the understorey of a subtropical eucalypt forest. Plant Soil 410 (1), 181–191. https://doi.org/10.1007/s11104-016-2995-x.

Cavallero, L., López, D., Raffaele, E., Aizen, M., 2015. Structural-functional approach to identify post-disturbance recovery indicators in forests from northwestern Patagonia: a tool to prevent state transitions. Ecol. Indic. 52, 85–95. https://doi.org/10.1016/J.ECOLIND.2014.11.019.

Chazdon, R., Broadbent, E., Rozendaal, D., Bongers, F., Zambrano, A., Aide, T., Balvanera, P., Becknell, J., Boukili, V., Brancalion, P., Craven, D., Almeida-Cortez, J., Cabral, G., Jong, B., Denslow, J., Dent, D., DeWalt, S., Dupuy, J., Durán, S., Espírito-Santo, M., Fandino, M., César, R., Hall, J., Hernández-Stefanoni, J., Jakovac, C., Junqueira, A., Kennard, D., Letcher, S., Lohbeck, M., Martínez-Ramos, M., Massoca, P., Meave, J., Mesquita, R., Mora, F., Muñoz, R., Muscarella, R., Nunes, Y., Ochoa-Gaona, S., Orihuela-Belmonte, E., Peña-Claros, M., Pérez-García, E., Piotto, D., Powers, J., Rodríguez-Velázquez, J., Romero-Pérez, I., Ruíz, J., Saldarriaga, J., Sánchez-Azofeifa, A., Schwartz, N., Steininger, M., Swenson, N., Uriarte, M., Breugel, M., Wal, H., Veloso, M., Vester, H., Vieira, I., Bentos, T., Williamson, G., Poorter, L., 2016. Carbon sequestration potential of second-growth forest regeneration in the Latin American tropics. Sci. Adv. 2. https://doi.org/10.1126/sciadv.1501639.

Chen, Q., Meng, Z., Liu, X., Jin, Q., Su, R., 2018. Decision variants for the automatic determination of optimal feature subset in RF-RFE. Genes (Basel) 9. https://doi.org/10.3390/genes9060301.

Chuvieco, E., Aguado, I., Salas, J., García, M., Yebra, M., Oliva, P., 2020. Satellite remote sensing contributions to wildland fire science and management. Curr. For. Rep. 6, 81–96. https://doi.org/10.1007/s40725-020-00116-5.

De Caceres, M., Jansen, F., De Caceres, M.M., 2016. Package 'indicspecies. Indicators 8 (1).

Dempewolf, J., Trigg, S., DeFries, R.S., Eby, S., 2007. Burned-area mapping of the Serengeti–Mara region using MODIS reflectance data. IEEE Geosci. Remote Sens. Lett. 4 (2), 312–316. https://doi.org/10.1109/LGRS.2007.894140.

Derroire, G., Balvanera, P., Castellanos-Castro, C., Decocq, G., Kennard, D., Lebrija-Trejos, E., Leiva, J., Odén, P., Powers, J., Rico-Gray, V., Tigabu, M., Healey, J., 2016. Resilience of tropical dry forests – a meta-analysis of changes in species diversity and composition during secondary succession. Oikos 125, 1386–1397. https://doi.org/10.1111/OIK.03229.

Fawzy, S., Osman, A.I., Doran, J., Rooney, D.W., 2020. Strategies for mitigation of climate change: a review. Environ. Chem. Lett. 18, 2069–2094.

Fernández-Guisuraga, J.M., Suárez-Seoane, S., Calvo, L., 2019. Modeling Pinus pinaster forest structure after a large wildfire using remote sensing data at high spatial resolution. For. Ecol. Manage. 446, 257–271. https://doi.org/10.1016/j.foreco.2019.05.028.

Filipponi, F., 2018. BAIS2: burned area index for Sentinel-2. In: Proceedings, 2. MDPI, p. 364. https://doi.org/10.3390/ecrs-2-05177.

Ford, A., Hardesty, B., 2012. Species adaptation to both fire and climate change in tropical montane heath: can Melaleuca uxorum (Myrtaceae) survive? Pacific Conserv. Biol. 18, 319–324. https://doi.org/10.1071/PC120319.

García, M.L., Caselles, V., 1991. Mapping burns and natural reforestation using Thematic Mapper data. Geocarto Int. 6 (1), 31–37. https://doi.org/10.1080/10106049109354290.

Gerard, F., Plummer, S., Wadsworth, R., Sanfeliu, A.F., Iliffe, L., Balzter, H., Wyatt, B., 2003. Forest fire scar detection in the boreal forest with multitemporal spot-vegetation data. IEEE Trans. Geosci. Remote Sens. 41 (11), 2575–2585. https://doi.org/10.1109/TGRS.2003.819190.

Gitelson, A.A., Gritz, Y., Merzlyak, M.N., 2003. Relationships between leaf chlorophyll content and spectral reflectance and algorithms for non-destructive chlorophyll assessment in higher plant leaves. J. Plant Physiol. 160 (3), 271–282. https://doi.org/10.1078/0176-1617-00887.

Gitelson, Kaufman, Y.J., Merzlyak, M.N., 1996. Use of a green channel in remote sensing of global vegetation from EOS-. MODIS, Remote Sens. Environ. 58, 289–298.

Gitelson, A., Merzlyak, M.N., 1994. Spectral reflectance changes associated with autumn senescence of aesculus hippocastanum L. and Acer platanoides L. Leaves. Spectral features and relation to chlorophyll estimation. J. Plant Physiol. 143 (3), 286–292. https://doi.org/10.1016/S0176-1617(11)81633-0.

González, M.E., 2005. Fire history data as reference information in ecological restoration. Dendrochronologia 22 (3), 149–154.

Han, A., Qing, S., Bao, Y., Na, L., Bao, Y., Liu, X., Zhang, J., Wang, C., 2021. Short-term effects of fire severity on vegetation based on Sentinel-2 satellite data. Sustainability 13 (1), 432.

Han, J., Shen, Z., Li, Y., Luo, C., Xu, Q., Yang, K., Zhang, Z., 2018. Beta diversity patterns of post-fire forests in central Yunnan Plateau, southwest China: disturbances intensify the priority effect in the community assembly. Front. Plant Sci. 9, 1000.

Hill, M.J., 2013. Vegetation index suites as indicators of vegetation state in grassland and savanna: an analysis with simulated SENTINEL 2 data for a North American transect. Remote Sens. Environ. 137, 94–111. https://doi.org/10.1016/j.rse.2013.06.004.

Holden, Z.A., Morgan, P., Hudak, A.T., 2010. Burn severity of areas reburned by wildfires in the Gila National Forest, New Mexico, USA. Fire Ecol. 6 (3), 77–85. https://doi.org/10.4996/fireecology.0603085.

Huang, Y.-L., Devan, M.N., U'Ren, J.M., Furr, S.H., Arnold, A.E., 2016. Pervasive effects of wildfire on foliar endophyte communities in montane forest trees. Microb. Ecol. 71, 452–468.

Imbert, J.B., Blanco, J.A., Candel-Pérez, D., Lo, Y.-H., González de Andrés, E., Yeste, A., Herrera-Álvarez, X., Rivadeneira Barba, G., Liu, Y., & Chang, S.-C. (2021). Synergies between climate change, biodiversity, ecosystem function and services, indirect drivers of change and human well-being in forests. Exploring Synergies and Trade-Offs between Climate Change and the Sustainable Development Goals, 263–320.

João, T., João, G., Bruno, M., João, H., 2018. Indicator-based assessment of post-fire recovery dynamics using satellite NDVI time-series. Ecol. Indic. 89, 199–212. https://doi.org/10.1016/j.ecolind.2018.02.008.

Kelley, D., Bistinas, I., Whitley, R., Burton, C., Marthews, T., Dong, N., 2019. How contemporary bioclimatic and human controls change global fire regimes. Nat. Clim. Chang. 1–7. https://doi.org/10.1038/s41558-019-0540-7.

Kilawe, C.J., Kaaya, O.E., Kolonel, C.P., Macrice, S.A., Mshama, C.P., Lyimo, P.J., Emily, C.J., 2021. Wildfires in the Eastern Arc Mountains of Tanzania: burned areas, underlying causes and management challenges. Afr. J. Ecol. 59 (1), 204–215.

Leutner, B., Horning, N., Leutner, M.B., 2017. Package 'RStoolbox'. R Foundation for Statistical Computing, Version 0.1.

Liu, S., Zheng, Y., Dalponte, M., Tong, X., 2020. A novel fire index-based burned area change detection approach using Landsat-8 OLI data. Eur. J. Remote Sens. 53 (1), 104–112. https://doi.org/10.1080/22797254.2020.1738900.

Lovett, J.C., 1996. Elevational and latitudinal changes in tree associations and diversity in the Eastern Arc mountains of Tanzania. J. Trop. Ecol. 12 (5), 629–650.

Liu, H.Q., Huete, A., 1995. A feedback based modification of the NDVI to minimize canopy background and atmospheric noise. IEEE Trans. Geosci. Remote Sens. 33 (2), 457–465. https://doi.org/10.1109/36.377946.

Lu, D., Batistella, M., Moran, E., de Miranda, E.E., 2008. A comparative study of Landsat TM and SPOT HRG images for vegetation classification in the Brazilian Amazon. Photogramm. Eng. Remote Sensing 74 (3), 311–321. https://doi.org/10.14358/PERS.74.3.311.

Majumdar, K., Choudhary, B., Datta, B., 2016. Changes of woody species diversity, horizontal and vertical distribution of stems across interior to outside within a primate rich habitat of Northeast India. J. For. Res. 27, 787–798. https://doi.org/10.1007/s11676-016-0231-4.

McGregor, H., Colloff, M., Lunt, I., 2016. Did early logging or changes in disturbance regimes promote high tree densities in river red gum forests. Aust. J. Bot. 64, 530–538. https://doi.org/10.1071/BT16025.

Miller, J., Thode, A., 2007. Quantifying burn severity in a heterogeneous landscape with a relative version of the delta normalized burn ratio (dNBR). Remote Sens. Environ. 109, 66–80. https://doi.org/10.1016/J.RSE.2006.12.006.

Mishra, V., Prasad, R., Rai, P., Vishwakarma, A., Arora, A., 2018. Performance evaluation of textural features in improving land use/land cover classification accuracy of heterogeneous landscape using multi-sensor remote sensing data. Earth Sci. Inform. 12, 71–86. https://doi.org/10.1007/s12145-018-0369-z.

Mondal, N., Sukumar, R., 2015. Regeneration of juvenile woody plants after fire in a seasonally dry tropical forest of Southern India. Biotropica 47. https://doi.org/10.1111/btp.12219.

Mori, A., Lertzman, K., Gustafsson, L., 2017. Biodiversity and ecosystem services in forest ecosystems: a research agenda for applied forest ecology. J. Appl. Ecol. 54, 12–27. https://doi.org/10.1111/1365-2664.12669.

Morris, R., 2010. Anthropogenic impacts on tropical forest biodiversity: a network structure and ecosystem functioning perspective. Philos. Trans. R. Soc. B: Biol. Sci. 365, 3709–3718. https://doi.org/10.1098/rstb.2010.0273.

Oliveras, I., Malhi, Y., Salinas, N., Huamán, V., Urquiaga-Flores, E., Kala-Mamani, J., Quintano-Loaiza, J., Cuba-Torres, I., Lizarraga-Morales, N., Roman-Cuesta, R., 2014. Changes in forest structure and composition after fire in tropical montane cloud forests near the Andean treeline. Plant Ecol. Divers. 7, 329–340. https://doi.org/10.1080/17550874.2013.816800.

Oliveras, I., Roman-Cuesta, R., Urquiaga-Flores, E., Loayza, J., Kala, J., Huamán, V., Lizárraga, N., Sans, G., Quispe, K., López, E., Lopez, D., Torres, I., Enquist, B., Malhi, Y., 2018. Fire effects and ecological recovery pathways of tropical montane cloud forests along a time chronosequence. Glob. Chang. Biol. 24, 758–772. https://doi.org/10.1111/gcb.13951.

Oksanen, J., Kindt, R., Legendre, P., O'Hara, B., Stevens, M.H.H., Oksanen, M.J., & Suggests, M. (2007). The vegan package. Community Ecology Package, 10 (631–637), 719.

Pearson, R.L., Milton, L.D., 1972. Remote mapping of standing crop biomass for estimation of the productivity of the shortgrass prairie, Pawnee National Grasslands, Colorado. In: Proceedings of the Eighth International Symposium on Remote Sensing of Environment, 1972.

Pinedo-Escatel, J.A., Aragón-Parada, J., Dietrich, C.H., Moya-Raygoza, G., Zahniser, J.N., Portillo, L., 2021. Biogeographical evaluation and conservation assessment of arboreal leafhoppers in the Mexican Transition Zone biodiversity hotspot. Divers. Distrib. 27 (6), 1051–1065.

Prichard, S.J., Hessburg, P.F., Hagmann, R.K., Povak, N.A., Dobrowski, S.Z., Hurteau, M. D., Kane, V.R., Keane, R.E., Kobziar, L.N., Kolden, C.A., 2021. Adapting western North American forests to climate change and wildfires: 10 common questions. Ecol. Appl. 31 (8), e02433.

Ranghetti, L., Boschetti, M., Nutini, F., Busetto, L., 2020. sen2r": An R toolbox for automatically downloading and preprocessing Sentinel-2 satellite data. Comput. Geosci. 139, 104473.

Richardson, A.J., Wiegand, C.L., 1977. Distinguishing vegetation from soil background information. Photogramm. Eng. Remote Sens. 43, 1541–1552.

Riley, K.L., Loehman, R.A., 2016. Mid-21st-century climate changes increase predicted fire occurrence and fire season length, Northern Rocky Mountains, United States. Ecosphere 7 (11), e01543.

Rurangwa, M.L., Aguirre-Gutiérrez, J., Matthews, T.J., Niyigaba, P., Wayman, J.P., Tobias, J.A., Whittaker, R.J., 2021. Effects of land-use change on avian taxonomic, functional and phylogenetic diversity in a tropical montane rainforest. Divers. Distrib. 27 (9), 1732–1746.

Rouse, J.W., Haas, R.H., Schell, J.A., Deering, D.W., 1974. Monitoring vegetation systems in the great plains with Erts, NASA special publication. Proceedings of the Third Earth Resources Technology Satellite- 1 Symposium, pp. 309–317.

Rodrigues, Santos, A, P., 2020. Prospects For Tropical Forest Biodiversity in the Landscapes of Southwestern Ethiopia: Conservation in a Context of Land Use Change and Human Population Growth. Leuphana Universität Lüneburg, Lüneburg. Dissertation.

Shin, Y.-J., Midgley, G.F., Archer, E.R., Arneth, A., Barnes, D.K., Chan, L., Hashimoto, S., Hoegh-Guldberg, O., Insarov, G., Leadley, P., 2022. Actions to halt biodiversity loss generally benefit the climate. Glob. Chang. Biol. 28 (9), 2846–2874.

Shuman, J.K., Balch, J.K., Barnes, R.T., Higuera, P.E., Roos, C.I., Schwilk, D.W., Stavros, E.N., Banerjee, T., Bela, M.M., Bendix, J., 2022. Reimagine fire science for the Anthropocene. PNAS Nexus 1 (3), 115 pgac.

Singh, S., 2022. Forest fire emissions: a contribution to global climate change. Front. For. Glob. Change 5, 925480.

Subashree, K., Dar, J., Karuppusamy, S., Sundarapandian, S., 2020. Plant diversity, structure and regeneration potential in tropical forests of Western Ghats, India. Acta Ecol. Sin. https://doi.org/10.1016/j.chnaes.2020.02.004.

Teixeira, A., Curran, T., Jameson, P., Meurk, C., Norton, D., 2020. Post-fire resprouting in New Zealand woody vegetation: implications for restoration. Forests. https://doi.org/10.3390/f11030269.

Trigg, S., Flasse, S., 2001. An evaluation of different bi-spectral spaces for discriminating burned shrub-savannah. Int. J. Remote Sens. 22 (13), 2641–2647. https://doi.org/10.1080/01431160110053185.

Tyukavina, A., Potapov, P., Hansen, M.C., Pickens, A.H., Stehman, S.V., Turubanova, S., Parker, D., Zalles, V., Lima, A., Kommareddy, I., 2022. Global trends of forest loss due to fire from 2001 to 2019. Front. Remote Sens. 3, 825190.

Wilcox, K., Koerner, S., Hoover, D., Borkenhagen, A., Burkepile, D., Collins, S., Hoffman, A., Kirkman, K., Knapp, A., Strydom, T., Thompson, D., Smith, M., 2020. Rapid recovery of ecosystem function following extreme drought in a South African savanna-grassland. Ecology. https://doi.org/10.1002/ecy.2983.

Zhang, N., Chen, M., Yang, F., Yang, C., Yang, P., Gao, Y., Shang, Y., Peng, D., 2022. Forest height mapping using feature selection and machine learning by integrating multi-source satellite data in Baoding City, North China. Remote Sens. (Basel) 14 (18), 4434.

Zvoleff, A. (2020). Package 'glcm'. *Calculate Textures from Grey-Level Co-Occurence Matrices (GLCMs)*. Available online: https://cran. r-project. org/web/packages/glcm/index. html (accessed on 25 October 2022).